# Free Liquid Surface Response Induced by Fluctuations of Thermal Marangoni Convection

Helmut F. Bauer*
*University of the German Armed Forces, Munich, Federal Republic of Germany*

**The original enthusiasm for processing in a microgravity environment has been slightly dimmed by the fact that liquid bridges are susceptible to surface oscillations and Marangoni convection. It has now been found that time fluctuations in the temperature gradient induce free liquid surface oscillations, which lead to large amplitudes in the vicinity of the resonances and possibly to the disintegration of the liquid system. An analytical solution leading to the magnification functions and phases of velocity, pressure distribution, and surface elevation is presented for an arbitrary axially periodic temperature field.**

## Nomenclature

$a$ = radius of liquid column
$f(z)$ = function of angular coordinate $z$ ($f' = df/dz$)
$I_0, I_1$ = modified Bessel function of zeroth and first order and first kind, respectively
$p$ = liquid pressure
$r, \varphi, z$ = cylindrical polar coordinates
$s$ = $\bar{\sigma} + i\bar{\omega}$ = complex frequency
$s_0$ = $i\bar{\omega}$ = frequency for inviscid liquid
$t$ = time
$T$ = temperature ($T_0, T_1$)
$u, w$ = velocity distribution
$\omega$ = natural frequency of frictionless liquid
$\Omega$ = forcing frequency of timewise temperature fluctuation
$\sigma$ = surface tension
$\rho$ = liquid density
$\eta$ = dynamic viscosity
$\nu$ = $\eta/\rho$ = kinetic viscosity
$\tau$ = shear stress
$\zeta$ = liquid surface elevation
$\Psi$ = stream function

## Introduction

THROUGH extended manned flight in a space laboratory, prolonged periods of a microgravity environment are achieved for experiments and unique manufacturing processes. Thus, for instance, was the floating zone technique pioneered on some of the Skylab flights,[1,2] where crystal growth experiments were performed with some success. This is done by heating one side of the feed material and cooling the other (crystal), such that the material in between exists in liquified form. It means that the system is subjected to a temperature gradient field.[3-5] This fact and other possibilities of the microgravity environment and the advantage of not needing a crucible for melts created a great deal of enthusiasm for such processes, where special emphasis was placed upon cylindrical liquid bridges. The hydrostatic behavior of such a liquid bridge in a microgravity environment yields much more stability and may make possible work with liquid columns of much larger diameter-to-length ratios. Crystal growth exhibited more homogeneous and striationless products. In the meantime, this optimism has been dimmed by the development of the so-called thermal Marangoni effect.[6,7] This is due to the absolutely necessary temperature gradient for the melting of the feed material and the cooling of the final crystal, which applied to the liquid surface creates a variation in surface tension.

Therefore, by viscous traction a conventional flow inside the liquid occurs. In addition, the susceptibility of the liquid to vibrational disturbances, such as $g$ jitter, control of the space laboratory, crew motion, or the operation of the on-board machines, enhances the displacement of the free liquid surface. These surface waves[8,9] will have a more or less detrimental effect upon the processes performed. It is therefore important to know the range of the natural frequencies[8] and their damping[9] in order to minimize their effects when experiments are performed. There is, however, an interaction of both effects, such that for a time-oscillatory temperature gradient field the free liquid surface is excited to perform surface oscillations, which exhibit large amplitudes in the vicinity of the resonances of the liquid bridge that could lead to the disintegration of the liquid system. Such time-oscillatory temperature gradients may, for instance, easily appear as a consequence of a fluctuating energy supply during heating. Since analytical solutions of a liquid bridge of finite length have not yet been obtained, we must resort to an infinitely long liquid bridge with a periodicity in the axial direction. Such a liquid bridge does not satisfy the boundary conditions at the ends of the floating zone, which would be $u = w = 0$, but does satisfy the vanishing of the axial velocity ($w = 0$) and a slip condition in the radial direction at the $z$ locations [see Eqs. (24) and (25) for $z = \lambda/4$ and $5\lambda/4$]. In addition, the effect of the aspect ratio $\lambda/a$ may be evaluated by such an axially dependent assumption. Therefore, it is believed that the analytical solution presented here yields a fairly good approximation of a finite liquid bridge and may be quite useful for many of the laboratory processes on a manned space flight.

This paper investigates the combined effect of liquid oscillations and Marangoni convection caused by a time-oscillatory temperature gradient in axial direction for an axisymmetric liquid column ($\partial/\partial\varphi = 0$). The magnification functions and phases for the velocity and pressure distributions as well as for the free surface elevation are presented in analytical form.

## Basic Equations and Solution

Under the influence of an axisymmetric and axially periodic temperature field applied as a time-harmonic fluctuation to the free surface of an infinite viscous liquid column, the liquid will not only exhibit internally a convection field due to the thermal Marangoni effect, but will also show a free liquid

Received July 14, 1982; revision received May 9, 1983. 

*Professor, Institute of Space Technology.

surface displacement from its circular cylindrical equilibrium position, which may be close to the resonances yielding large amplitudes. To solve this interaction problem we assume axial symmetry ($\partial/\partial\varphi=0$), creeping flow, and incompressible liquid. Therefore, the linearized Navier-Stokes equations (see Fig. 1)

$$\frac{\partial u}{\partial t}+\frac{1}{\rho}\frac{\partial p}{\partial r}=\nu\left[\frac{\partial^2 u}{\partial r^2}+\frac{1}{r}\frac{\partial u}{\partial r}-\frac{u}{r^2}+\frac{\partial^2 u}{\partial z^2}\right] \tag{1}$$

$$\frac{\partial w}{\partial t}+\frac{1}{\rho}\frac{\partial p}{\partial z}=\nu\left[\frac{\partial^2 w}{\partial r^2}+\frac{1}{r}\frac{\partial w}{\partial r}+\frac{\partial^2 w}{\partial z^2}\right] \tag{2}$$

have to be solved with the continuity equation

$$\frac{\partial u}{\partial r}+\frac{u}{r}+\frac{\partial w}{\partial z}=0 \tag{3}$$

and the appropriate boundary conditions at the free liquid surface $r=a+\zeta$.

The Navier-Stokes equations have been linearized in order to obtain an analytical solution. The analysis is thus valid for creeping flow and therefore particularly useful for checking numerical computer solutions in the limit case of small Reynolds numbers. The boundary conditions will be described by the normal and shear stress, i.e., $\tau_{rr}$ and $\tau_{rz}$. The normal stress is equal to the surface tension pressure and yields, with $\zeta$ as the free surface elevation for the axisymmetric case,

$$p-2\eta\frac{\partial u}{\partial r}=\frac{\sigma}{a}-\frac{\sigma}{a^2}\left[\zeta+a^2\frac{\partial^2\zeta}{\partial z^2}\right] \text{ at } r=a \tag{4}$$

The bracket in this expression is essential for liquid surface oscillations. The shear stress $\tau_{rz}$ with the Marangoni effect ($\bar{\tau}=\text{grad}\,\sigma=\mathrm{d}\sigma/\mathrm{d}T\cdot\text{grad}\,T$) is given by

$$\tau_{rz}=\eta\left[\frac{\partial u}{\partial z}+\frac{\partial w}{\partial r}\right]=\frac{\mathrm{d}\sigma}{\mathrm{d}T}\frac{\partial T}{\partial z} \text{ at } r=a \tag{5}$$

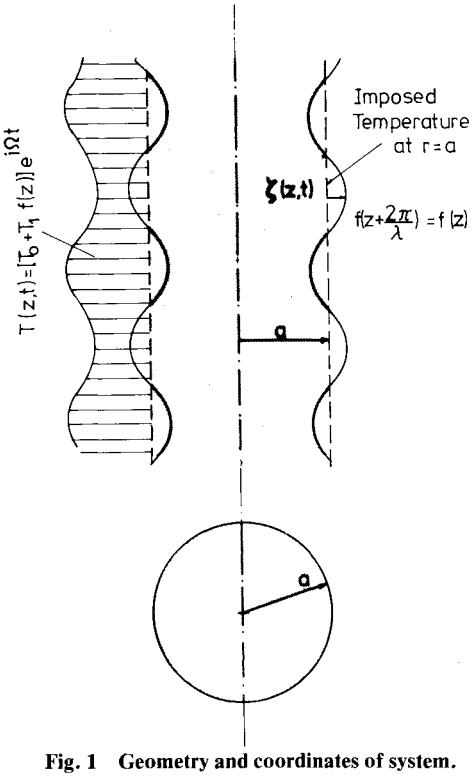


**Fig. 1 Geometry and coordinates of system.**

The kinematic boundary condition in linearized form is given by

$$u=\frac{\partial\zeta}{\partial t} \text{ at } r=a \tag{6}$$

The value $\sigma$ represents the liquid surface tension, $\zeta$ the free liquid surface elevation, and $T$ the temperature field $T(z,t)$ imposed upon the free liquid surface. The latter condition is a result of the variation in the surface temperature caused by the dependence of the surface tension upon the temperature flow force from colder to warmer regions.

Introducing the stream function $\Psi$, which satisfies continuity equation (3), i.e.,

$$u=\frac{1}{r}\frac{\partial\Psi}{\partial z} \text{ and } w=-\frac{1}{r}\frac{\partial\Psi}{\partial r} \tag{7}$$

yields the well-known differential equation of the stream function

$$\bar{\Delta}\left[\bar{\Delta}\Psi-\frac{1}{\nu}\frac{\partial\Psi}{\partial t}\right]=0 \tag{8}$$

where the operator $\bar{\Delta}$ is given by

$$\bar{\Delta}\equiv\frac{\partial^2}{\partial r^2}-\frac{\partial}{r\partial r}+\frac{\partial^2}{\partial z^2}$$

Assuming an imposed temperature field at the free liquid surface of the form

$$T(z,t)=[T_0+T_1 f(z)]e^{i\Omega t} \text{ or } T(z,t)=T_0+T_1 f(z)e^{i\Omega t} \tag{9}$$

where $\Omega$ represents the forcing frequency and $f(z)$ a periodic function of the axial coordinate $z$ with the period $\lambda=2\pi/k$ ($\lambda$ is the wavelength and $k$ the wave number), the temperature gradient may be expressed in the form

$$\frac{\partial T}{\partial z}=T_1 e^{i\Omega t}\sum_{m=1}^{\infty}\left[f_m\cos(mkz)+g_m\sin(mkz)\right] \tag{10}$$

where $f_m$ and $g_m$ are given by

$$f_m=\frac{k}{\pi}\int_{-\pi/k}^{+\pi/k}f'(z)\cos(mkz)\,\mathrm{d}z$$

$$g_m=\frac{k}{\pi}\int_{-\pi/k}^{+\pi/k}f'(z)\sin(mkz)\,\mathrm{d}z \tag{11}$$

The solution of Eq. (8) is

$$\Psi(r,z,t)=e^{i\Omega t}\sum_{m=1}^{\infty}\left[rI_1(mkr)\{A_m\cos(mkz)+B_m\sin mkz\}\right.$$
$$\left.+\{C_m\cos(mkz)+D_m\sin mkz\}rI_1\left(\sqrt{m^2k^2+\frac{i\Omega}{\nu}}\,r\right)\right] \tag{12}$$

where $I_1$ is the modified Bessel function of first order and first kind. The integration constants $A_m$, $B_m$, $C_m$, and $D_m$ are determined from the boundary conditions [Eqs. (4-6)]. Taking the divergence operation upon Navier-Stokes equations (1) and (2) yields the Laplace equation for pressure

$$\Delta p=\frac{\partial^2 p}{\partial r^2}+\frac{1}{r}\frac{\partial p}{\partial r}+\frac{\partial^2 p}{\partial z^2}=0 \tag{13}$$

The pressure distribution inside the liquid is therefore given by

$$p(r,z,t) = \frac{\sigma}{a} + \sum_{m=1}^{\infty} I_0(kmr)\,[F_m \cos(kmz) + E_m \sin(kmz)]\, e^{i\Omega t} \tag{14}$$

Introducing the previous results into the Navier-Stokes equations yields the relations for the constants

$$E_m = i\Omega\rho A_m \quad \text{and} \quad F_m = -i\Omega\rho B_m \tag{15}$$

The boundary conditions [Eqs. (4-6)] at the free liquid surface yield the relations for the determination of the remaining constants. After the introduction of Eqs. (15) and (6) into the timewise differentiated equation (4) and after separating the sine and cosine terms, these relations are

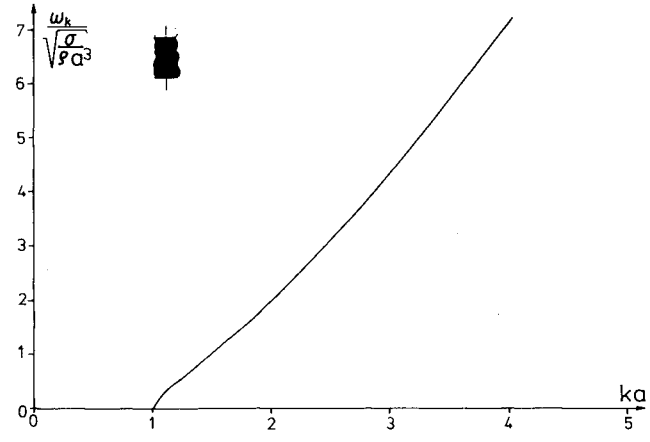


**Fig. 2 Undamped axisymmetric natural frequencies of liquid column.**

$$B_m\left[\Omega^2 I_0(kma) - 2\frac{\nu}{a^2}k^2m^2a^2 i\Omega I_1'(kma) + \frac{\sigma kma}{\rho a^3}(1-k^2a^2m^2)\cdot I_1(kma)\right] + D_m\left[\frac{\sigma kma}{\rho a^3}(1-k^2a^2m^2) I_1\left(\sqrt{k^2m^2+\frac{i\Omega}{\nu}}\,a\right)\right.$$
$$\left. - 2\frac{\nu}{a^2} i\Omega kma\sqrt{k^2m^2a^2+\frac{i\Omega}{\nu}a^2}\, I_1\left(\sqrt{k^2m^2+\frac{i\Omega}{\nu}}\,a\right)\right] = 0 \tag{16}$$

$$-A_m\left[\Omega^2 I_0(kma) - 2\frac{\nu}{a^2} i\Omega k^2m^2a^2 I_1'(kma) + \frac{\sigma kma}{\rho a^3}(1-k^2a^2m^2) I_1(kma)\right] + C_m\left[2\frac{\nu}{a^2} i\Omega kma\sqrt{k^2m^2a^2+\frac{i\Omega}{\nu}a^2}\, I_1'\left(\sqrt{k^2m^2+\frac{i\Omega}{\nu}}\,a\right)\right.$$
$$\left. - \frac{\sigma kma}{\rho a^3}(1-k^2a^2m^2) I_1\left(\sqrt{k^2m^2+\frac{i\Omega}{\nu}}\,a\right)\right] = 0 \tag{17}$$

For the shear stress condition we obtain

$$A_m 2k^2m^2a^2 I_1(kma) + C_m I_1\left(\sqrt{k^2m^2+\frac{i\Omega}{\nu}}\,a\right)\left[2k^2m^2a^2+\frac{i\Omega}{\nu}a^2\right] = -\frac{a^2}{\eta}\frac{d\sigma}{dT}T_1 f_m \tag{18}$$

$$B_m 2k^2m^2a^2 I_1(kma) + D_m I_1\left(\sqrt{k^2m^2+\frac{i\Omega}{\nu}}\,a\right)\left[2k^2m^2a^2+\frac{i\Omega}{\nu}a^2\right] = -\frac{a^2}{\eta}\frac{d\sigma}{dT}T_1 g_m \tag{19}$$

From these equations the values of $A_m$, $B_m$, $C_m$, and $D_m$ may be obtained as functions of the temperature-forcing frequency $\Omega$. The velocity distribution is, therefore,

$$u(r,z,t) = e^{i\Omega t}\sum_{m=1}^{\infty}\left\{mkI_1(mkr)\,[B_m(\Omega)\cos(mkz) - A_m(\Omega)\sin(mkz)]\right.$$
$$\left. + mkI_1\left(\sqrt{m^2k^2+\frac{i\Omega}{\nu}}\,r\right)[D_m(\Omega)\cos(kmz) - C_m(\Omega)\sin(mkz)]\right\} \tag{20}$$

and

$$w(r,z,t) = -e^{i\Omega t}\sum_{m=1}^{\infty}\left\{mkI_0(kmr)\,[A_m(\Omega)\cos(mkz) + B_m(\Omega)\sin(mkz)] + \sqrt{m^2k^2+\frac{i\Omega}{\nu}}\,I_0\left(\sqrt{k^2m^2+\frac{i\Omega}{\nu}}\,r\right)\right.$$
$$\left.\times\,[C_m(\Omega)\cos(mkz) + D_m(\Omega)\sin(mkz)]\right\} \tag{21}$$

while the pressure may be obtained from Eqs. (14) and (15). The free liquid surface elevation $\zeta$ above the equilibrium position $r=a$ is given, using Eq. (6), by

$$\zeta(z,t) = \frac{-2e^{i\Omega t}}{\Omega}\sum_{m=1}^{\infty}\left\{mkI_1(mka)\,[B_m(\Omega)\cos(mkz) - A(\Omega)\sin mkz] + mkI_1\left(\sqrt{k^2m^2+\frac{i\Omega}{\nu}}\,a\right)[D_m(\Omega)\cos(mkz) - C_m(\Omega)\sin(mkz)]\right\} \tag{22}$$

The axial displacement at the free surface may be obtained with the same approximation from $\xi(z,t) = w(a,z,t)/i\Omega$.

It may be seen from the result that the liquid responds to the time-oscillatory excitation via the Marangoni effect with a phase-shifted motion. The above procedure may also be applied to any timewise periodic function of the temperature. In this case, the applied temperature distribution [Eq. (9)] may be substituted by

$$T(z,t) = \mathrm{Re}\sum_{n=1}^{\infty}\{T_{0n} + T_{1n}f(z)\}e^{in\Omega t}$$

where Re denotes the real part (see Ref. 10 for a similar treatment) and $T_{jn} = T_{jn}^{*} - iT_{jn}^{**}$.

## Special Case

We consider the special case of an applied temperature distribution in the form (see Fig. 1)

$$T(z,t) = e^{i\Omega t}[T_0 + T_1 \sin kz] \quad \text{or} \quad T(z,t) = T_0 + T_1 e^{i\Omega t}\sin kz \tag{23}$$

With this the axial tempeature gradient yields $\partial T/\partial z = T_1 k \cos kz e^{i\Omega t}$, i.e.,

$$f_1 = k, \quad g_1 = 0, \quad \text{and} \quad f_m = g_m = 0 \quad \text{for all } m > 1$$

The velocity distribution is then presented by

$$u(r,z,t) = -e^{i\Omega t}\left\{A_1(\Omega)kI_1(kr) + C_1(\Omega)kI_1\left(\sqrt{k^2 + \frac{i\Omega}{\nu}}\,r\right)\right\}\sin kz \tag{24}$$

$$w(r,z,t) = -e^{i\Omega t}\left\{A_1(\Omega)kI_0(kr) + C_1(\Omega)\sqrt{k^2 + \frac{i\Omega}{\nu}}\,I_0\left(\sqrt{k^2 + \frac{i\Omega}{\nu}}\,r\right)\right\}\cos kz \tag{25}$$

while the free surface elevation and the pressure distribution are given by

$$\zeta(z,t) = \frac{kie^{i\Omega t}}{\Omega}\left\{A_1(\Omega)I_1(ka) + C_1(\Omega)I_1\left(\sqrt{k^2 + \frac{i\Omega}{\nu}}\,a\right)\right\}\sin kz \tag{26}$$

and

$$p(r,z,t) = \sigma/a + i\Omega\rho A_1(\Omega)I_0(kr)\sin kz e^{i\Omega t} \tag{27}$$

The constants $A_1(\Omega)$ and $C_1(\Omega)$ are obtained from

$$A_1\left[\Omega^2 I_0(ka) - \frac{2\nu}{a^2}i\Omega k^2 a^2 I_1'(ka) + \frac{\sigma ka}{\rho a^3}(1-k^2a^2)I_1(ka)\right] - C_1\left[\frac{2\nu}{a^2}i\Omega ka\sqrt{k^2a^2 + \frac{i\Omega}{\nu}a^2}\,I_1'\left(\sqrt{k^2 + \frac{i\Omega}{\nu}}\,a\right) - \frac{\sigma ka}{\rho a^3}(1-k^2a^2)I_1\left(\sqrt{k^2 + \frac{i\Omega}{\nu}}\,a\right)\right] = 0 \tag{28a}$$

and

$$A_1 2kaI_1(ka)\frac{\nu}{a^2} + C_1\frac{[2k^2a^2 + (i\Omega/\nu)a^2]}{ka} \times I_1\left(\sqrt{k^2 + \frac{i\Omega}{\nu}}\,a\right)\frac{\nu}{a^2} = -\frac{d\sigma}{dT}\frac{T_1}{\rho a} \tag{28b}$$

Finally, introducing the values $A_1(\Omega)$ and $C_1(\Omega)$ into the velocity distributions [Eqs. (24) and (25)] as well as into the free liquid surface displacement [Eq. (26)] and the pressure distribution [Eq. (27)] enables us to present them as magnification functions, i.e., amplitudes as a function of the forcing frequency $\Omega$ and their phases. For this special case, these will be evaluated numerically and presented in graphical form.

## Numerical Evaluation and Conclusions

The undamped natural frequencies (Fig. 2) for the axisymmetric case of an infinite frictionless liquid column $(\partial/\partial\varphi = 0)$ is given by[8,11]

$$\omega_k^2 = (\sigma ka/\rho a^3)(k^2a^2 - 1)I_1(ka)/I_0(ka) \tag{29}$$

which expresses that for $ka < 1$, i.e., a wavelength $\lambda > 2\pi a$, the column is not stable. For viscous liquid, the damped natural frequency is obtained from[9,12]

$$I_1(x)\left\{x^6 I_0(ka) + x^4[k^2a^2 I_0(ka) - 2kaI_1(ka)] + x^2\left[4k^3a^3 I_1(ka) - k^4a^4 I_0(ka) - \frac{\sigma a}{\rho\nu^2}(1-k^2a^2)kaI_1(ka)\right] + k^6a^6 I_0(ka) - 2k^5a^5[kaI_0(ka) + I_1(ka)] + \frac{\sigma a}{\rho\nu^2}k^3a^3 \times (1-k^2a^2)I_1(ka)\right\} = 4k^3a^3 I_1(ka)x(x^2 - k^2a^2)I_0(x) \tag{30}$$

with $x = \sqrt{(sa^2/\nu) + k^2a^2}$ and $s = \sigma + i\omega$ as the complex frequency. $s_0$ is the root for the inviscid liquid.

The result of the evaluation of this expression is presented in Fig. 3 for the oscillatory root for various tension parameters $\sigma/\rho a^3$ and viscosity parameters $\nu/a^2$. The real and imaginary parts of $sa^2/\nu$ are presented. The value $s_0a^2/\nu$ is the root of the frictionless liquid. We see that this root possesses only an imaginary part that decreases with the decreasing wave number parameter $ka > 1$ to zero at $ka = 1$, at which point the roots appear as stable and instable real parts. For a viscous liquid, the oscillatory root exhibits a smaller imaginary part and a negative real part, indicating that the oscillation of the liquid surface is decaying as time goes on. With decreasing $ka$ the conjugate complex root decreases the magnitude of the real and imaginary parts until the imaginary part vanishes at a $ka$ value larger than unity. This root pair then splits into two negative real roots of decaying magnitude until one assumes at $ka = 1$ a positive value, indicating instability. This shows that for a viscous liquid a decrease in the range of oscillatory motion is obtained in the range of $ka$ values above unity. This means that the damped oscillation is

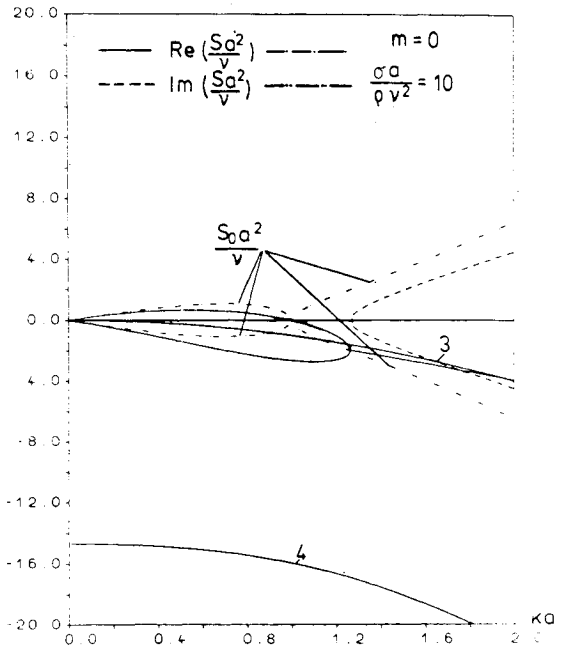


**Fig. 3 Damped axisymmetric roots of liquid column as function of wave number parameter $ka$.**

stable for a wavelength of $\lambda < 2\pi a$, i.e., smaller than the circumference of the column. For even smaller $ka$ values ($ka < 1.27$), the motion remains stable for another short range of $ka$ ($1.0 < ka < 1.27$), although the oscillatory character has ceased to exist. For $ka = 1.0$ the system is unstable.

Figure 4 shows the oscillatory root in the complex frequency plane ($s$ plane) for varying $ka$ and $\sigma a/\rho\nu^2$ values. With the increasing wave number parameter $ka \geq 1.27$, the root increases its imaginary and negative real parts, indicating that for a larger $ka$ value (i.e., smaller wavelength) the natural damped frequency increases, while the oscillation decays much faster. For increased tension parameter $\sigma/\rho a^3$, the oscillation frequency increases with a slight increase in the decay magnitude. Increased viscosity indicates a stronger decay of the oscillation. For a wavelength $\lambda$ smaller than the circumference, the oscillation is decreased and is accompanied by a stronger decay.

For the case of interaction of oscillatory Marangoni effect and free liquid surface elevation, some numerical results are presented in Figs. 5-7 for various surface tension parameters $\sigma/\rho a^3$, viscosity parameters $\nu/a^2$, and wave number parameters $ka$. The radial velocities $u$ at $r/a = 1$ are shown in Fig. 5, where the magnification functions are presented by solid lines and the phases by dashed lines. In Fig. 5a the radial velocity $u$ is shown for an axial wavelength $\lambda = 2\pi/k = \pi a$ ($ka = 2$), which has the magnitude of half the circumference of the liquid column. The viscosity parameter is $\nu/a^2 = 0.2$, while the surface tension parameter $\sigma/\rho a^3$ exhibits values of 10, 20, and 50. For these values the undamped natural frequency $\omega_k$ assumes the values of 6.47, 9.15, and 14.47 $s^{-1}$, respectively. They are indicated by the vertical bar on the forcing frequency axis $\Omega$. The magnification functions show their peak values very close to the natural frequencies $\omega_k$. They shift with increasing surface tension parameter $\sigma/\rho a^3$ toward larger forcing frequency $\Omega$ values. The magnitude of the peak in the radial velocity $u$ does not show any appreciable change as a function of the surface tension parameter. In resonance the phases exhibit a shift of the magnitude $\pi$ and assume, with increasing forcing frequency $\Omega$, a value from $-\pi/2$ to $-3\pi/2$, while the magnification of $u$ decreases above resonance as $\Omega$ increases toward zero. In Fig. 5b the effect of the viscosity parameter $\nu/a^2$, ranging 0.05-0.5, is shown for $ka = 2$ and at $r/a = 1$ for $\sigma/\rho a^3 = 10$. The radial velocity shows its peak in relation to $\omega_k$ [Eq. (29)] near these values. It may be noticed that, with decreasing axial wavelength $\lambda = 2\pi/k$, the magnitude of the peak of the radial velocity decreases slightly and exhibits larger magnitudes over a wider band of forcing frequencies. The radial velocity $u$ inside the column is, of course, of smaller magnitude than that at the surface itself.

The response of the axial velocity $w$ is shown in Fig. 6 for the same parameters as in the previous case. Again we notice that the peak of the magnification of $w$ shifts with increasing surface tension parameter $\sigma/\rho a^3$ toward larger $\Omega$ values and does not appreciably change its magnitude. The peak for the axial velocity (as may be seen for the radial velocity) is shifted for $r/a = 1$ toward larger $\Omega$ values compared to $\omega_k$. The phase for $w$ remains around $\pi$. The influence of the viscosity parameter $\nu/a^2$ upon the axial velocity is shown in Fig. 6b, where increasing viscosity decreases the magnitude of the response in the axial velocity and a shift (at $r = a$) of the peak value toward larger $\Omega$ values. In Fig. 6c we may see the effect

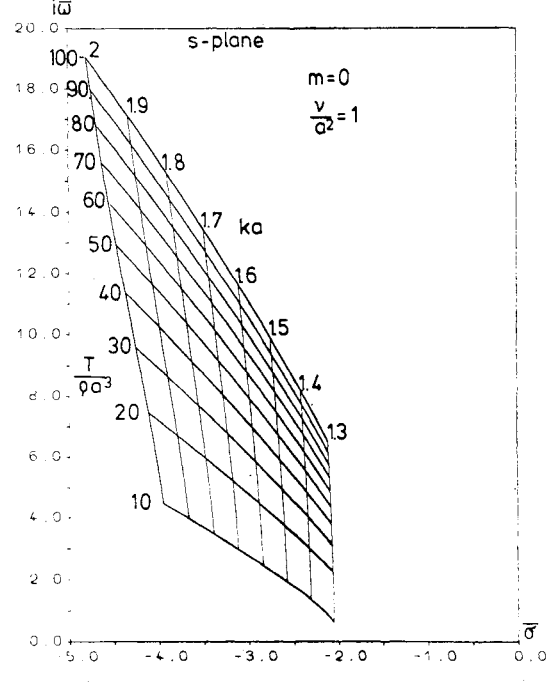


Fig. 4 Damped axisymmetric oscillatory root for $\sigma/\rho a^3 = 10$.

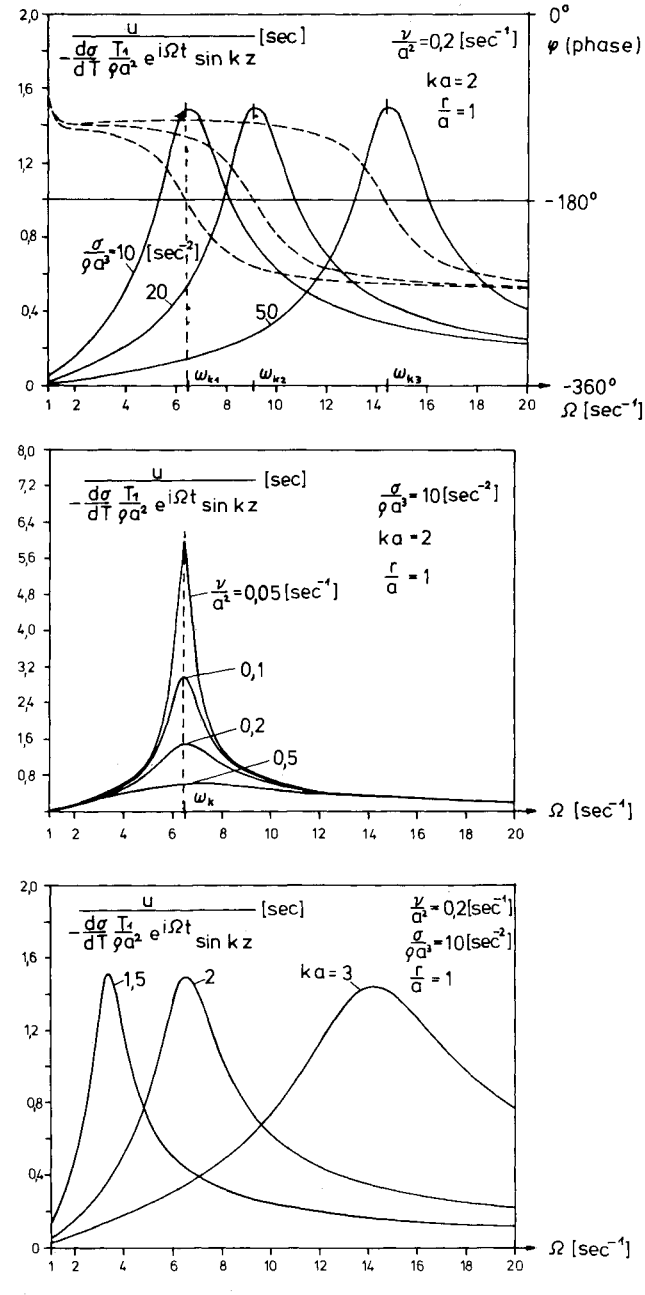


Fig. 5 Radial velocity distribution: magnification function and phase.

of the wave number parameter $ka$, which shows for increasing wave number a decrease of the peak at a larger forcing frequency $\Omega$ and a much flatter response for smaller wavelengths. The axial velocity $w$ at smaller $r/a$ values shows much smaller peak values.

In Fig. 7 we finally represent the response of the free liquid surface displacement $\zeta$. The influence of the surface tension parameter $\sigma/\rho a^3$ is exhibited in Fig. 7a. With increasing surface tension the magnitude of the peak decreases and shifts toward larger values of forcing frequency $\Omega$. The peak values appear at smaller $\Omega$ values compared to $\omega_k$ ($\Omega_{\text{peak}} < \omega_k$). The influence of the viscosity parameter $\nu/a^2$ is presented in Fig. 7b for $\sigma/\rho a^3 = 10\ \text{s}^{-2}$ and $ka = 2$. Again we notice that, with increasing $\nu$ or decreasing diameter of the liquid column, the peak magnitude decreases strongly and shifts to $\Omega < \omega_k$. With the increasing forcing frequency of the temperature gradient, the free liquid surface amplitude decreases toward zero. Finally, Fig. 7c shows the influence of the wave number parameter $ka$. The increase of the wave number (i.e., a decrease of the axial wave length $\lambda = 2\pi/k$) shows a considerable decrease of the peak free surface amplitude occurring at a larger magnitude of the forcing frequency $\Omega$. It may, however, be noticed that the peak becomes much flatter. From these numerical evaluations we may conclude that a disintegration of the liquid column due to large free liquid surface amplitudes may occur not only for axial wavelengths larger than the circumference of the liquid column as in the frictionless case, but also through oscillatory temperature gradients that, due to the thermal Marangoni effect, excite the otherwise calm free liquid surface. Such large-amplitude free surface elevations may occur at small forcing frequencies of the imposed fluctuations on the temperature gradient for small surface tension $\sigma$, large density $\rho$, small viscosity $\nu$, long axial waves $\lambda$ (i.e., small $k$), and even more so for large diameters of the liquid column. For wavelengths larger than the circumference of the liquid column, the system is already hydrodynamically unstable.

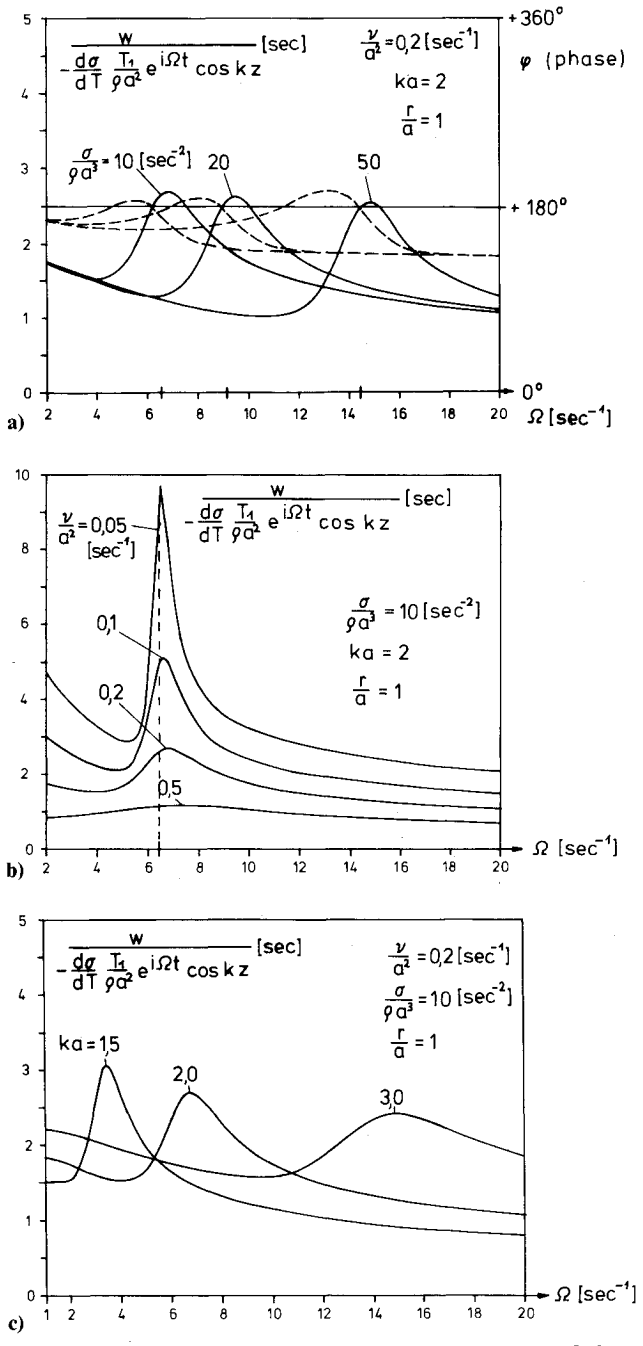


Fig. 6 Axial velocity distribution: magnification function and phase.

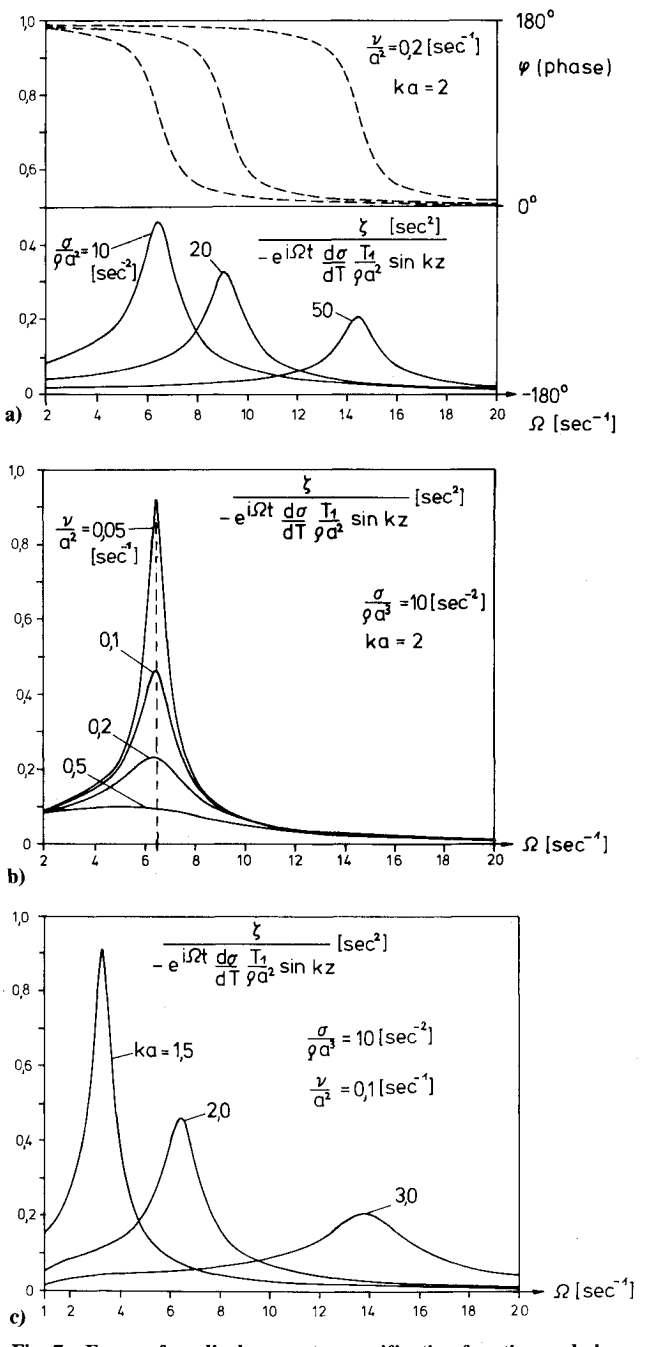


Fig. 7 Free surface displacement: magnification function and phase.

## Remarks

The importance of temperature gradients as a cause of convective instability has been well established by Pearson[13] and Sternling and Scriven,[14,15] while in later work by the latter the surface was considered deformable with capillary waves possible on it. Smith[16] then investigated the linearized stability problem for steady, cellular convection resulting from gradients in the surface tension and showed that in thin layers a critical Marangoni number is assured. It should also be mentioned that it can be shown experimentally[17,18] that the Marangoni convection becomes oscillatory at higher Marangoni numbers, and that there seems to exist a critical number. Schwabe and Scharmann[17] found good agreement with the results of Chun and Wuest.[18] Their experiments revealed that steady Marangoni convection is stable only below a certain critical Marangoni number, beyond which a transition into an oscillatory convection takes place due to the growing of temperature disturbances traveling around the free surface of a floating zone. A reasonable assumption for the cause of this instability of the steady laminar convection may well be a temperature perturbation on the free surface of the liquid column. Such a coupling mechanism of the thermal Marangoni effect and the free surface waves has been studied above and it can be definitely shown that a temperature disturbance may grow and create an oscillatory field if the disturbance of the imposed temperature field remains oscillatory. It results (depending on the forcing frequency) in large or small response amplitudes according to the magnitude of $\Omega$ close to or away from the surface wave resonances. Large amplitudes of the surface displacement and the involved liquid velocities at or near the resonances possibly result first in a turbulent flow and finally in a disintegration of the floating zone. However, it may be noticed that then a nonlinear theory of the problem will give more accurate details and conclusions about the possibly softening behavior of the system and the instability regions of the floating zone.

There seems to exist, however, another coupling mechanism in which a temperature disturbance on the surface of the zone leads, due to the additional variation of the surface tension, to a corresponding disturbance of the velocity distribution inside the floating zone and consequently to a change of the temperature field inside the zone and again on its free liquid surface. This coupling mechanism could make a small temperature perturbation decay or grow, depending on a characteristic value that seems to be the Marangoni number. It could be defined as

$$Mg = c\left|\frac{\mathrm{d}\sigma}{\mathrm{d}T}\right|\frac{a(T_1 - T_2)}{\nu\kappa}$$

where $|\mathrm{d}\sigma/\mathrm{d}T|$ is the temperature coefficient of the surface tension, $a$ the radius of the liquid column, $\nu$ its kinematic viscosity, $c$ the specific heat, $\kappa$ the thermal conductivity, and $(T_1 - T_2)$ the temperature difference between the upper and lower boundary of the floating zone. An oscillatory effect can, however, already be shown for a mere forced temperature oscillation upon the floating system's free liquid surface, for which the above-mentioned coupling mechanism between the surface tension gradient and the heat transfer was neglected. Therefore, there may be two different ways to induce an oscillatory Marangoni convection, one being created by forced time-oscillatory temperature gradients and the other by a disturbance at an increased Marangoni number.

## Appendix

In the previously treated case, we considered an axial temperature gradient proportional to a Fourier series in $z$ with the period $\lambda = 2\pi/k$. The method employed may easily be extended to exponential axial dependency, for which just the stream function and the equations for the determination of the response functions $A(\Omega)$ and $B(\Omega)$ are represented. From these the response of the radial and axial velocities, as well as the free surface elevation $\zeta$, may easily be obtained. For a temperature distribution

$$T = [T_0 + T_1 e^{-\lambda z}]e^{i\Omega t} \quad \text{or} \quad T = T_0 + T_1 e^{-\lambda z} e^{i\Omega t}$$

the stream function is given by[10]

$$\Psi(r,z,t) = e^{i\Omega t}\left[ArJ_1(\lambda r) + BrJ_1\left(\sqrt{\lambda^2 - \frac{i\Omega}{\nu}}\, r\right)\right]e^{-\lambda z}$$

To determine the response for that exponential axial temperature distribution the values $A(\Omega)$ and $B(\Omega)$ as obtained from the dynamic and kinematic conditions, as well as the shear stress condition at the free liquid surface, have to be obtained from

$$A\left\{2i\Omega\lambda^2 a^2\left(\frac{\nu}{a^2}\right)J_1'(\lambda a) - \Omega^2 - \frac{\sigma\lambda a}{\rho a^3}(1+\lambda^2 a^2)J_1(\lambda a)\right\}$$

$$+B\left\{2i\Omega\lambda a\left(\frac{\nu}{a^2}\right)\sqrt{\lambda^2 a^2 - \frac{i\Omega a^2}{\nu}}\,J_1'\left(\sqrt{\lambda^2 a^2 - \frac{i\Omega a^2}{\nu}}\right)\right.$$

$$\left.-\frac{\sigma\lambda a}{\rho a^3}(1+\lambda^2 a^2)J_1\left(\sqrt{\lambda^2 a^2 - \frac{i\Omega a^2}{\nu}}\right)\right\} = 0$$

and

$$2A\left(\frac{\nu}{a^2}\right)\lambda^2 a^2 J_1(\lambda a) + B\left(\frac{\nu}{a^2}\right)\left[2\lambda^2 a^2\right.$$

$$\left.-\frac{i\Omega a^2}{\nu}\right]J_1\left(\sqrt{\lambda^2 a^2 - \frac{i\Omega a^2}{\nu}}\right) = -\frac{\lambda a T_1}{\rho a}\frac{\mathrm{d}\sigma}{\mathrm{d}T}$$

## References


[1] *Proceedings of the Third Space Processing Symposium, Skylab Results*, April 30-May 1, 1974, NASA Rept. M.75.5, 1974.

[2] Grodzka, P. G. and Bannister, T. C., "Heat Flow and Convection Demonstration Experiments Aboard Apollo 14," *Science*, Vol. 176, May 1972, pp. 506-508.

[3] Carruthers, J. R., Gibson, E. G., Klett, M. G., and Facemire, B. R., "Studies of Rotating Liquid Floating Zones on Skylab IV," AIAA Paper 75-692, May 1975.

[4] Chun, Ch.-H., "Marangoni Convection in a Floating Zone under Reduced Gravity," *Journal of Crystal Growth*, Vol. 48, 1980, pp. 600-610.

[5] Wuest, W., "Fluid Dynamics of a Floating Zone," *Proceedings of the Second European Symposium on Material Sciences in Space*, Frascati, Italy, April 1976, ESA SP-114, Sept. 1976, pp. 455-465.

[6] Scriven, L. E. and Sternling, C. V., "The Marangoni Effects," *Nature*, Vol. 187, 1960, pp. 186-188.

[7] Bauer, H. F., "Velocity Distribution due to Thermal Marangoni Effect in a Liquid Column under Zero-Gravity Environment," *ZAMM*, Vol. 62, 1982, pp. 471-482.

[8] Bauer, H. F., Coupled Oscillations of a Solidly Rotating Liquid Bridge, *Acta Astronautica*, Vol. 9, No. 9, 1982, pp. 547-563.

[9] Bauer, H. F., "Natural Damped Frequencies of an Infinitely Long Column of Immiscible Viscous Liquids, Part II: Three-Dimensional Case," Forschungsbericht HSBw:LRT-WE-9-FB-1, 1982.

[10] Bauer, H. F., "Marangoni Effect Velocity Distribution Due to Time-Oscillatory Temperature Gradients in Zero-Gravity Environment," *Acta Mechanica*, Vol. 46, 1983, pp. 167-187.

[11] Lamb, H., *Hydrodynamics*, Dover Publications, New York, 1945, pp. 471-473.

[12]Bauer, H. F., "Natural Damped Frequencies of an Infinitely Long Column of Immiscible Viscous Liquids, Part I: Two-Dimensional and Axisymmetric Case," Forschungsbericht HSBw:LRT-WE-9-FB-2, 1982.

[13]Pearson, J.R.A., "On Convective Cells Induced by Surface Tension," *Journal of Fluid Mechanics*, Vol. 4, 1958, pp. 489-497.

[14]Scriven, L. E. and Sternling, L. V., "On Cellular Convection Driven by Surface Tension Gradients: Effects of Mean Surface Tension and Surface Viscosity," *Journal of Fluid Mechanics*, Vol. 19, 1964, pp. 321-332.

[15]Sternling, L. V. and Scriven, L. E., "Interfacial Turbulence: Hydrodynamic Instability and the Marangoni Effect," *AIChE Journal*, Vol. 6, 1959, pp. 514-519.

[16]Smith, K. A., "On Convective Instability Induced by Surface Tension Gradients," *Journal of Fluid Mechanics*, Vol. 24, Pt. 2, 1966, pp. 401-414.

[17]Schwabe, D. and Scharmann, A., "Some Evidence for the Existence and Magnitude of a Critical Marangoni Number for the Onset of Oscillatory Flow in Crystal Growth Melts," *Journal of Crystal Growth*, Vol. 46, 1979, pp. 125-131.

[18]Chun, Ch.-H. and Wuest, W., "Experiments on the Transition from a Steady to the Oscillatory Marangoni Convection of a Floating Zone under Reduced Gravity Effect," *Acta Astronautica*, Vol. 6, 1979, pp. 1073-1082.